ANTIOXIDANTS & REDOX SIGNALING
Volume 10, Number 3, 2008
© Mary Ann Liebert, Inc.
DOI: 10.1089/ars.2007.1865

Forum News & Views

Is Antioxidant Potential of the Mitochondrial Targeted Ubiquinone Derivative MitoQ Conserved in Cells Lacking mtDNA?

CHAO LU,[1] DAWEI ZHANG,[1] MATTHEW WHITEMAN,[2] and JEFFREY S. ARMSTRONG[1]

ABSTRACT

MitoQ has been developed as a mitochondrial targeted antioxidant for diseases associated with oxidative stress. Here we show that MitoQ blocks the generation of reactive oxygen species (ROS) and mitochondrial protein thiol oxidation, and preserves mitochondrial function and ultrastructure after glutathione (GSH) depletion. Furthermore, the antioxidant effect of MitoQ is conserved in cells lacking mitochondrial DNA, indicating that its antioxidant properties do not depend on a functional electron transport chain (ETC). Our results elucidate the antioxidant mechanism of MitoQ and suggest that it may be a useful therapeutic for disorders associated with a dysfunctional ETC and increased ROS production. *Antioxid. Redox Signal.* 10, 651–660.

MITOCHONDRIAL MEMBRANE PERMEABILIZATION REGULATES CELL DEATH

MITOCHONDRIA ARE PRINCIPAL SITES of intracellular reactive oxygen species (ROS) production and play an important role in cell death, which occurs when their membranes become permeabilized. Mitochondria possess two discrete membrane systems and both membranes can be involved in the permeabilization process. Whereas mitochondrial outer membrane permeabilization involves proteins of the Bcl-2 family and often leads to programmed cell death by apoptosis, inner membrane permeabilization is associated with the mitochondrial permeability transition (MPT) and cell death by necrosis (3). Although the MPT is a well-studied phenomenon, both its structure and regulation are controversial. One key factor regulating the MPT is the cellular redox environment (4, 10, 23), which is, in part, controlled by the tripeptide glutathione (GSH). Cellular depletion of GSH creates an increasingly oxidized environment in both the cytosol and the mitochondria with increased formation of mitochondrial ROS leading to mitochondrial permeabilization and cell death (4).

DEVELOPMENT OF MITOCHONDRIAL TARGETED UBIQUINONE DERIVATIVES AS ANTIOXIDANTS

Over recent years, a variety of pharmacological antioxidant strategies has been developed aimed at blocking ROS production in diseases where GSH levels are often found to be decreased (26). A number of these approaches are based on the use of the lipid-soluble antioxidant compound coenzyme Q (CoQ_{10}), a redox component of the mitochondrial electron transport chain (ETC). The antioxidant properties of CoQ_{10} depend, in part, on its redox-cycling from the oxidized (ubiquinone) form to the reduced (ubiquinol) form by the ETC (7, 11). However, the poor solubility of CoQ_{10} has precluded its general use and led to the development of shorter chain antioxidant CoQ_{10} derivatives, including the synthetic compound

[1]Department of Biochemistry, Yong Loo Lin School of Medicine, National University of Singapore, Republic of Singapore.
[2]Peninsula Medical School, Universities of Exeter and Plymouth, St Luke's Campus, Exeter, England.

idebenone (6-(10-hydroxydecyl)-2,3-dimethoxy-5-methyl-1,4-benzoquinone) and decylubiquinone (dUb) (12). To increase the specificity of targeting the antioxidant to the site of ROS production, mitochondrial targeted analogs of dUb, including the compound MitoQ, a triphenylphosphonium linked ubiquinone derivative, have been developed (21). MitoQ concentrates several hundred-fold within mitochondria, due to the large mitochondrial membrane potential ($\Delta\psi$m), with its alkyl chain in-

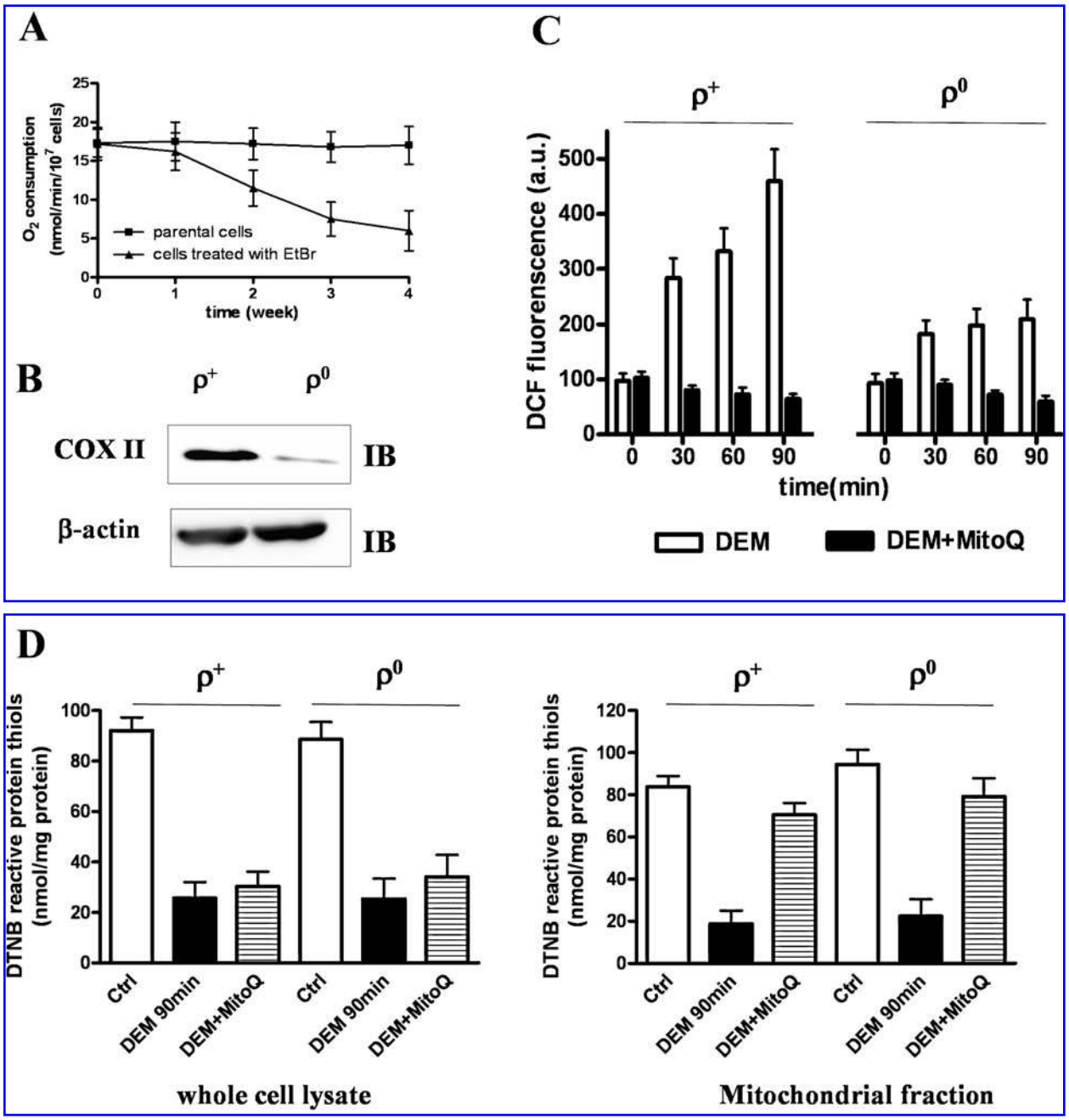

FIG. 1. MitoQ blocks oxidative stress after DEM treatment in both ρ^+ and ρ^0 cells. (**A**) Mean oxygen consumption rate of parental CEM cells compared to cells treated with 50 ng/ml EtBr at week 0, 1, 2, 3, and 4. The data are expressed as mean ± SEM ($n = 3$). (**B**) Western blot analysis of expression of cytochrome oxidase subunit II (COX II) in ρ^+ and ρ^0 cells. β-actin was used as loading control. (**C**) ρ^+ and ρ^0 cells (7×10^5/ml) were treated with DEM ± MitoQ for 0, 30, 60, and 90 min, washed in PBS, and suspended in PBS containing 10 m*M* glucose. Cells were loaded with 10 μM DCFDA for 15 min and mean DCF fluorescence (a.u.) recorded by FACS using FITC channel are shown as *bar graphs*. Representative example from at least three independent experiments. In each analysis, 10,000 events were recorded. Data are expressed as mean ± SEM ($n = 3$). (**D**) ρ^+ and ρ^0 cells (7×10^5/ml) were treated with RPMI (control) or DEM ± MitoQ for 90 min and DTNB reactive protein thiols in whole cell lysate (*left panel*) and mitochondrial fraction (*right panel*) were measured using Ellman's method and shown as *bar graphs*. Data are expressed as mean ± SEM ($n = 3$).

serted into the hydrophobic core of the inner membrane (27). The selective accumulation of MitoQ in mitochondria and its continual recycling by mitochondrial enzymes, including those of the ETC, have been suggested to make MitoQ a significantly more potent antioxidant than nontargeted antioxidants (20). In agreement with this, MitoQ has been shown to be cardioprotective in an *ex vivo* model of ischemia-reperfusion injury (1) and to protect against GSH-dependent oxidative stress in fibroblasts from patients with the neurodegenerative disorder Friedreich ataxia (15). Since defective mitochondrial DNA (mtDNA) and increased oxidative stress are common features of various neurodegenerative diseases, MitoQ may be a potentially useful therapeutic antioxidant (17). However, the antioxidant mechanism of MitoQ is not well understood and it is not known whether the compound's antioxidant potential is conserved in cells with defective mtDNA and dysfunctional ETC.

MITOQ BLOCKS ROS GENERATION, BUT NOT GSH DEPLETION, AFTER DEM TREATMENT IN ρ^+ AND ρ^0 CELLS

To investigate the antioxidant mechanism of MitoQ, we used diethylmaleate (DEM) to deplete GSH from parental human leukemic CEM cells (ρ^+) and from CEM cells lacking mtDNA (ρ^0). ρ^0 cells were generated by treating the parental CEM ρ^+ cells with 50 ng/ml ethidium bromide (EtBr) for ~4 weeks. Figure 1A shows mean oxygen consumption rate of parental cells and cells continuously treated with EtBr at week 0, 1, 2, 3, and 4. Results show that after EtBr treatment for 4 weeks, oxygen consumption was decreased ~90% ($p < 0.05$), indicating that the ETC was significantly compromised in these cells. A representative immunoblot of cytochrome oxidase subunit II (COX II) protein expression also shows that in ρ^0 cells the COX II subunit, which is encoded by mtDNA, showed ~90% decreased expression (Fig. 1B), indicating a significant reduction in the mtDNA content of the ρ^0 cell line which corresponded with the relative level of KCN-sensitive oxygen consumption that was observed in these cells.

GSH and GSSG (oxidized form of glutathione) levels and GSH redox potential (E_h) were determined on aliquots of ρ^+ and ρ^0 cells treated with DEM ± MitoQ. DEM treatment for 30 min significantly reduced total GSH levels in ρ^+ cells (from 65.1 ± 14.8 to 0.2 ± 0.06 nmol/mg protein, $p < 0.05$) and ρ^0 cells (from 68.9 ± 5.1 to 0.3 ± 0.07 nmol/mg protein, $p < 0.05$). Pretreatment of MitoQ did not prevent DEM-induced GSH depletion since GSH levels were 0.4 ± 0.02 nmol/mg protein in ρ^+ cells and 0.5 ± 0.02 nmol/mg protein in ρ^0 cells (Table 1). The GSH *Nernst* redox potential (E_h), compared to control cells, increased ~141 mV in ρ^+ cells treated with DEM and ~132 mV in ρ^+ cells treated with DEM + MitoQ; similarly, E_h increased ~140 mV in ρ^0 cells treated with DEM and ~132 mV in ρ^0 cells treated with DEM + MitoQ (Table 1).

Cellular oxidation and ROS production after DEM treatment were then determined by monitoring the fluorescence of the ROS sensitive dye DCF. Figure 1C shows mean DCF fluorescence (a.u.) recorded by FACS analysis. DEM treatment caused progressive increase in DCF fluorescence in both ρ^+ and ρ^0 cells, indicating increased ROS production. The ROS increase observed in ρ^0 cells was significantly reduced compared to ρ^+ cells. Pretreatment of MitoQ prevented the increase of DCF fluorescence in both cell lines, indicating that MitoQ was an effective antioxidant after DEM treatment in both ρ^+ and ρ^0 cells.

MITOQ PRESERVES MITOCHONDRIAL PROTEIN THIOL REDOX STATUS AFTER GSH DEPLETION IN ρ^+ AND ρ^0 CELLS

Intracellular protein thiol redox status of ρ^+ and ρ^0 cells was determined using Ellman's method of DTNB reactive protein thiols measurement. ρ^+ and ρ^0 cells were treated with RPMI (control), DEM ± MitoQ for 90 min, and DTNB reactive protein thiols in whole cell lysate (left panel) and mitochondrial fraction (right panel) were measured (Fig. 1D). DTNB reactive protein thiols in whole cell lysate and mitochondrial fractions from ρ^+ and ρ^0 cells treated with DEM were significantly reduced compared to controls ($p < 0.05$). Pretreatment of ρ^+ and ρ^0 cells with MitoQ did not prevent loss of protein thiol redox status in whole cell lysate but preserved mitochondrial protein thiol redox status of ρ^+ and ρ^0 cells indicating that MitoQ, which specifically targets to mitochondria, protected mitochondrial protein redox status after GSH depletion.

TABLE 1. GSH/GSSG AND E_h LEVELS IN CEM ρ^+ AND ρ^0 CELLS TREATED WITH DEM ± MITOQ

	Nernst GSH redox potential E_h *(mV)*		*Total GSH/GSSG (nmol/mg protein)*	
	ρ^+	ρ^0	ρ^+	ρ^0
Control	−264 ± 7.2	−267 ± 11.2	65.1 ± 14.8/1.2 ± 0.1	68.9 ± 5.4/1.4 ± 0.2
DEM	−123 ± 10.5	−127 ± 3.2	0.2 ± 0.06/0.9 ± 0.05	0.3 ± 0.07/0.9 ± 0.04
DEM + MitoQ	−132 ± 5.6	−144 ± 9.3	0.4 ± 0.02/1.1 ± 0.11	0.5 ± 0.02/1.1 ± 0.09

Aliquots (~ 4×10^6/ml) of ρ^+ and ρ^0 cells treated with RPMI (control), DEM, or DEM + MitoQ for 30 min, and GSH and GSSG concentrations were determined using a commercial assay kit described in the methods section. The GSH redox potential (E_h) in mV was calculated using the *Nernst* equation as described in the methods section. Data are expressed as mean ± SEM ($n = 3$).

MITOQ BLOCKS LOSS OF $\Delta\psi$m AND PRESERVES MITOCHONDRIAL ULTRASTRUCTURE AFTER GSH DEPLETION IN ρ^+ AND ρ^0 CELLS

To determine whether MitoQ preserved the functional and structural integrity of mitochondria after GSH depletion, mitochondrial membrane potential ($\Delta\psi$m) was determined by monitoring the fluorescence of cationic potentiometric dye TMRM. Figure 2A shows representative FACS two-dimensional color density plots of TMRM-stained cells showing percentage number of cells with intact $\Delta\psi$m (top right quadrant) versus percentage number of cells with reduced $\Delta\psi$m (bottom left quadrant). Figure 2B shows mean TMRM fluorescence (a.u.) of ρ^+ and ρ^0 cells recorded by FACS. Reduced percentage number of cells with intact $\Delta\psi$m as well as decreased mean TMRM fluorescence ($p < 0.05$) indicated that GSH depletion caused loss of $\Delta\psi$m which occurred at ~120 min in ρ^+ cells and 180 min in ρ^0 cells after DEM treatment. Pretreatment with MitoQ blocked loss of $\Delta\psi$m in both ρ^+ and ρ^0 cells, indicating that MitoQ preserved mitochondrial function after GSH depletion.

Mitochondrial ultrastructural (electron microscopic (EM)) analysis was performed on ρ^+ and ρ^0 cells treated with DEM ± MitoQ (Fig. 2C). Caption '1' shows mitochondrial structure from ρ^+ and ρ^0 control cells; inset arrowheads point to mitochondrial cristae. Caption '2' shows mitochondria of ρ^+ and ρ^0 cells treated with DEM; inset arrowheads point to fragmented electron dense mitochondria and vacuolated mitochondria. Caption '3' shows mitochondria of ρ^+ and ρ^0 cells treated with DEM + MitoQ; inset arrowheads point to mitochondrial cristae. The results show that pretreatment of ρ^+ and ρ^0 cells with MitoQ preserved the integrity of mitochondrial structure after GSH depletion.

MITOQ BLOCKS CASPASE-INDEPENDENT CELL DEATH AFTER GSH DEPLETION IN ρ^+ AND ρ^0 CELLS

Figure 3A shows representative cytochrome *c* immunoblot determined on cytosolic fractions taken from ρ^+ and ρ^0 cells treated with DEM for 0, 30, 60, 90, and 120 min or 1 μM staurosporine (STS) for 6 h which was included as positive control. The result shows that DEM treatment did not lead to the release of cytochrome *c* from the mitochondria to the cytosol. Figure 3B shows a bar graph of caspase-3 activity in ρ^+ and ρ^0 cells after treatment with DEM for 120 min or STS for 9 h. The result shows that caspase-3 was not activated after DEM treatment compared to treatment with STS. Figure 3C shows cell viability, determined by trypan blue exclusion, of ρ^+ and ρ^0 cells treated with RPMI (control), DEM, DEM + z-VADfmk (50 μM), STS, or STS + z-VADfmk. The result shows that z-VADfmk, a pan-caspase inhibitor, did not prevent DEM-induced cell death. Taken together, the data indicate that cell death after DEM treatment is caspase-independent. Figure 3D shows viability of ρ^+ and ρ^0 cells treated with RPMI (control), DEM ± MitoQ for 0, 30, 60, 90, 120, 150, 180, 210, and 240 min. MitoQ pretreatment blocked cell death after DEM treatment up to 240 min ($p < 0.05$).

COMPARISON OF THE ANTIOXIDANT EFFICACY OF MITOCHONDRIAL TARGETED AND NONTARGETED COENZYME Q DERIVATIVES IN ρ^+ AND ρ^0 CELLS

To compare the antioxidant efficacy of MitoQ with a nontargeted coenzyme Q derivative and to determine whether the antioxidant efficacy of MitoQ was similar in ρ^+ and ρ^0 cells, we treated cells with various concentrations of MitoQ (0.1–1,000,000 nM), MitoQ (0.1–1,000,000 nM)+ FCCP (10 μM) and dUb (0.1–1,000,000 nM) (Fig. 4A). Figure 4B shows concentrations of MitoQ, MitoQ + FCCP, and dUb that prevented 50% of cell death induced by DEM treatment (EC_{50}) in ρ^+ and ρ^0 cells. Results show that although dUb (EC_{50}: 623 ± 123 nM in ρ^+ cells and 786 ± 137 nM in ρ^0 cells) was able to block cell death, MitoQ (EC_{50}: 12 ± 5 nM in ρ^+ cells and 33 ± 13 nM in ρ^0 cells) were ~50-fold and ~20-fold more effective, respectively. Cotreatment of MitoQ with FCCP to depolarize the $\Delta\psi$m abolished the antioxidant efficacy of MitoQ (EC_{50}: 563 ± 134 nM in ρ^+ cells and 729 ± 145 nM in ρ^0 cells), indicating that the higher antioxidant efficacy of MitoQ was dependent on its accumulation into mitochondria driven by $\Delta\psi$m. Notably, the effectiveness of MitoQ was only observed to decrease slightly in ρ^0 cells. To investigate the potent antioxidant potential of MitoQ in ρ^0 cells, we semiquantitatively determined the relative $\Delta\psi$m of both ρ^+ and ρ^0 cells by measuring TMRM fluorescence. CEM ρ^+ cells and ρ^0 cells were incubated with

FIG. 2. MitoQ blocks loss of $\Delta\psi$m and preserves mitochondrial ultrastructure after GSH depletion. (**A**) Representative FACS two-dimensional color density plots of CEM cells stained with TMRM and analyzed using PE channel. Aliquots of ρ^+ and ρ^0 cells (7×10^5/ml) were treated with DEM ± MitoQ for 0, 60, 120, and 180 min, washed in PBS, and suspended in PBS containing 10 mM glucose. Cells were loaded with 250 nM TMRM for 15 min and the fluorescence was measured by flow cytometry. Percentage number of cells with intact $\Delta\psi$m (*top right quadrant*) and percentage number of cells with reduced $\Delta\psi$m (*bottom left quadrant*) are shown. Representative example from at least three independent experiments. In each analysis, 10,000 events were recorded. (**B**) Mean TMRM fluorescence (a.u.) of ρ^+ and ρ^0 cells recorded by FACS as described above. Data are expressed as mean ± SEM ($n = 3$). (**C**) Representative electron micrographs of ρ^+ and ρ^0 cells treated with RPMI (control) or DEM ± MitoQ for 120 min and 180 min, respectively. Caption '1' shows mitochondria in control cells; *inset arrowheads* point to mitochondrial cristae. Caption '2' shows mitochondria of cells treated with DEM; *inset arrowheads* point to fragmented electron dense mitochondria and vacuolated mitochondria. Caption '3' shows mitochondria of cells treated with DEM + MitoQ; *inset arrowheads* point to mitochondrial cristae. (For interpretation of the references to color in this figure legend, the reader is referred to the web version of this article at www.liebertonline.com/ars).

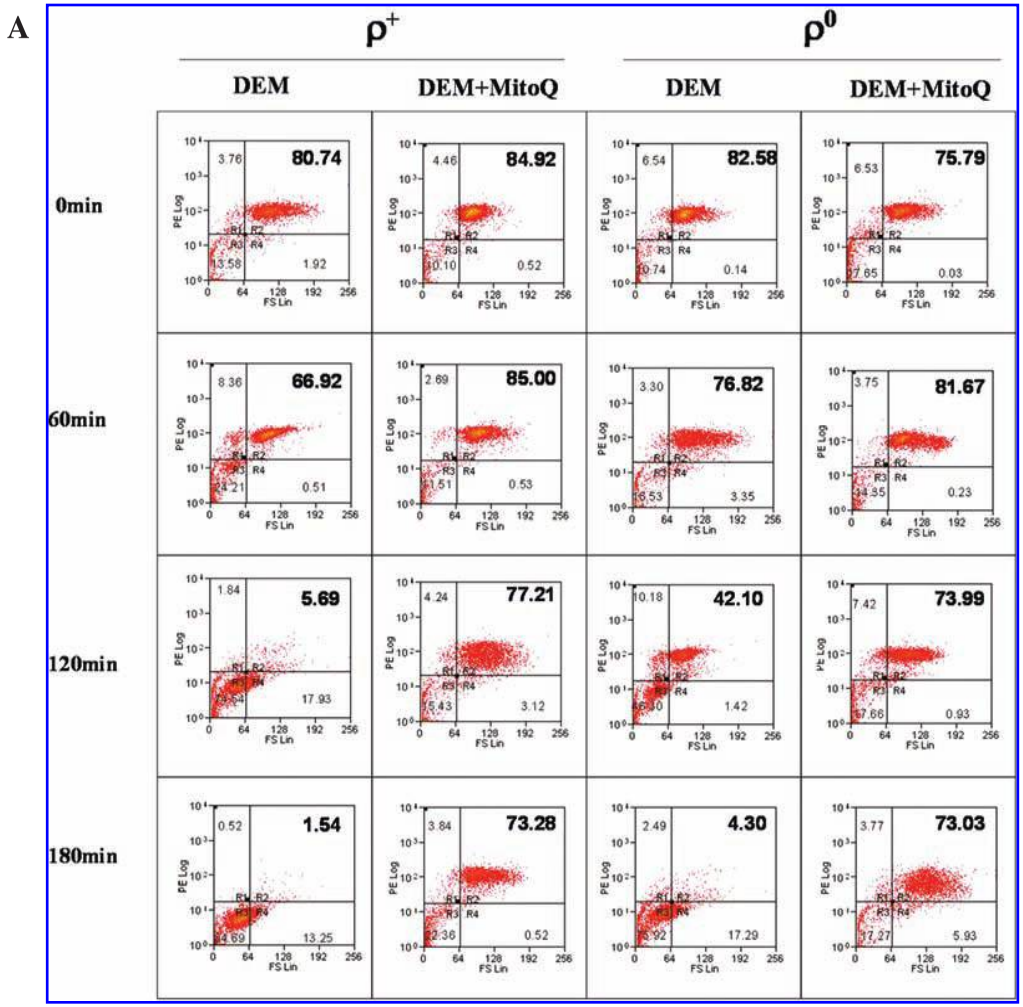
A
ρ+
ρ0
DEM
DEM+MitoQ
DEM
DEM+MitoQ
0min
60min
120min
180min
80.74
84.92
82.58
75.79
66.92
85.00
76.82
81.67
5.69
77.21
42.10
73.99
1.54
73.28
4.30
73.03
PE Log
FS Lin

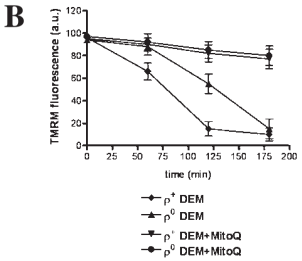
B
TMRM fluorescence (a.u.)
time (min)
ρ+ DEM
ρ0 DEM
ρ+ DEM+MitoQ
ρ0 DEM+MitoQ

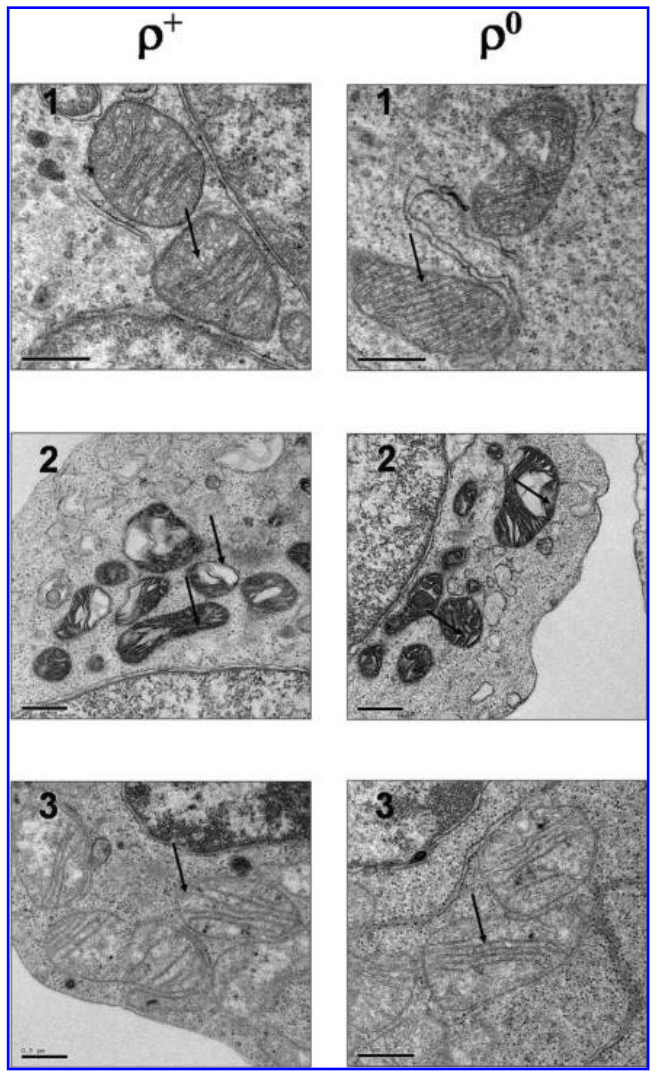
C
ρ+
ρ0
1
2
3

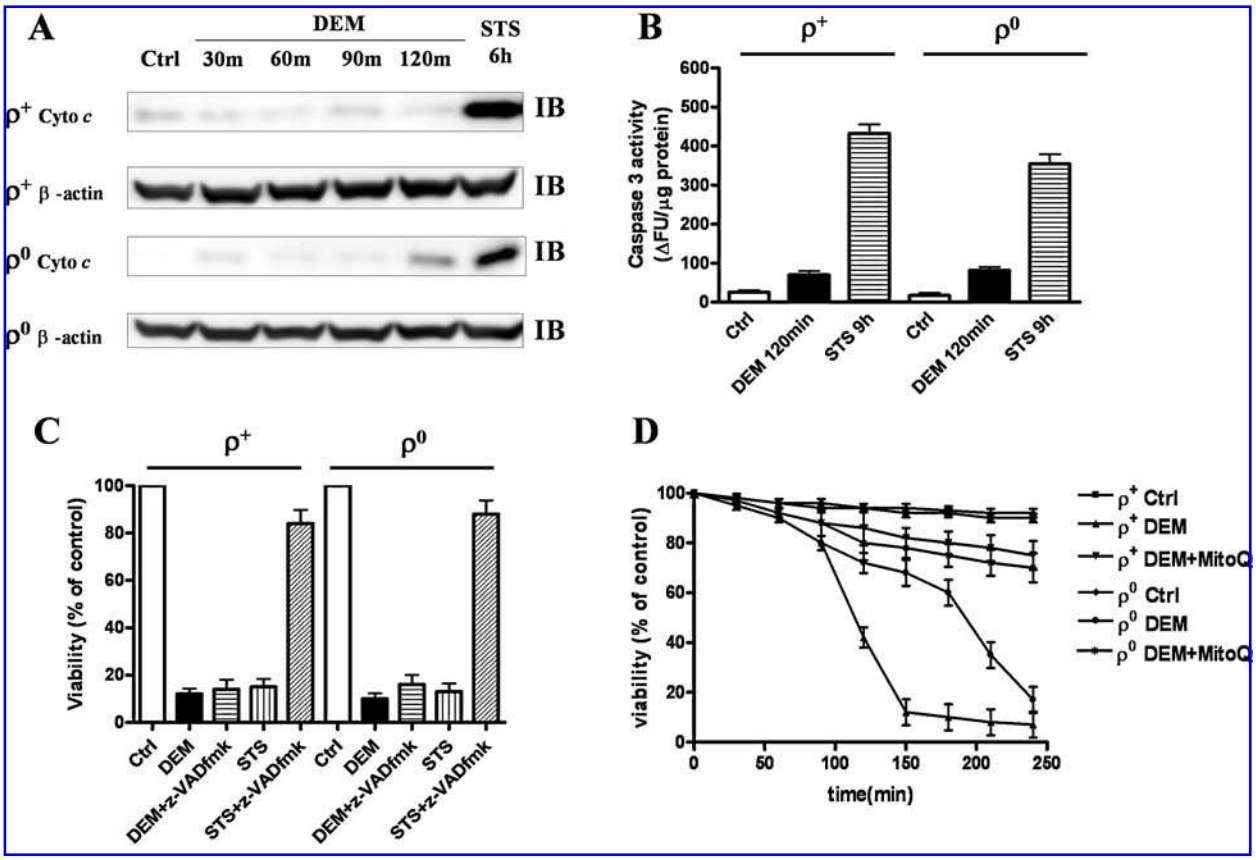

FIG. 3. MitoQ blocks caspase-independent cell death after GSH depletion. (**A**) Representative cytochrome *c* immunoblot determined on cytosolic fractions of ρ^+ and ρ^0 cells treated with DEM for 0, 30, 60, 90, 120 min or STS (1 μM) for 6 h which was included as positive control. β-Actin was used as loading control. (**B**) Bar graph of caspase-3 activity in ρ^+ and ρ^0 cells after treatment of DEM for 120 min or STS for 9 h. Data are expressed as mean ± SEM ($n = 3$). (**C**) ρ^+ and ρ^0 cells were treated with RPMI (control), DEM, DEM + z-VADfmk (50 μM), STS (1 μM), or STS + z-VADfmk, and cell viability was determined by trypan blue exclusion. Data are expressed as mean ± SEM ($n = 3$). (**D**) ρ^+ and ρ^0 cells were treated with RPMI (control), DEM and DEM + MitoQ, and cell viability was determined by trypan blue exclusion at 0, 30, 60, 90, 120, 150, 180, 210, and 240 min. Data are expressed as mean ± SEM ($n = 3$).

40 n*M* tetramethyl rhodamine methyl ester (TMRM) for 15 min. The $\Delta\psi$m of CEM ρ^+ cells was arbitrarily set to −130 mV and the $\Delta\psi$m of ρ^0 cells was determined using equation: −130 mV × log [fluorescence intensity of ρ^+ cells/no TMRM]/log [fluorescence intensity of ρ^0 cells/no TMRM] (24). $\Delta\psi$m of ρ^0 cells was determined to be approximately 20 mV lower (~ 110 mV) compared to ρ^+ cells (Fig. 4C).

ANTIOXIDANT POTENTIAL OF MITOQ IS CONSERVED IN CELLS LACKING MtDNA

The antioxidant mechanism of MitoQ has been previously studied in isolated mitochondria and in cell model systems where it has been shown to protect against oxidative damage. In isolated mitochondria, MitoQ was shown to detoxify super-

FIG. 4. Comparison of the antioxidant efficacy of mitochondrial targeted and nontargeted CoQ_{10} derivatives in ρ^+ and ρ^0 cells. (**A**) Viability of ρ^+ and ρ^0 cells after DEM treatment in the presence of various concentrations of MitoQ, MitoQ + FCCP (10 μM) or dUb determined by trypan blue exclusion. Data are expressed as mean ± SEM ($n = 5$). (**B**) Bar graphs showing the EC_{50} (effective concentration that prevents 50% of cell death) for MitoQ, MitoQ + FCCP (10 μM) and dUb in ρ^+ and ρ^0 cells. Data are expressed as mean ± SEM ($n = 5$). (**C**) Semiquantitative determination of $\Delta\psi$m in ρ^+ and ρ^0 cells. Cells were washed in PBS and suspended in PBS containing 10 m*M* glucose, loaded with 40 n*M* TMRM for 15 min, and TMRM fluorescence was measured by FACS analysis using PE channel. The $\Delta\psi$m of CEM ρ^+ cells was arbitrarily set to −130 mV and the $\Delta\psi$m of ρ^0 cells was determined using equation: −130mV × log [fluorescence intensity of ρ^+ cells/no TMRM]/log [fluorescence intensity of ρ^0 cell/no TMRM]. Data are expressed as mean ± SEM ($n = 3$). *Inset figure* shows representative FACS histograms of CEM cells stained with TMRM as described above. In each analysis, 10,000 events were recorded.

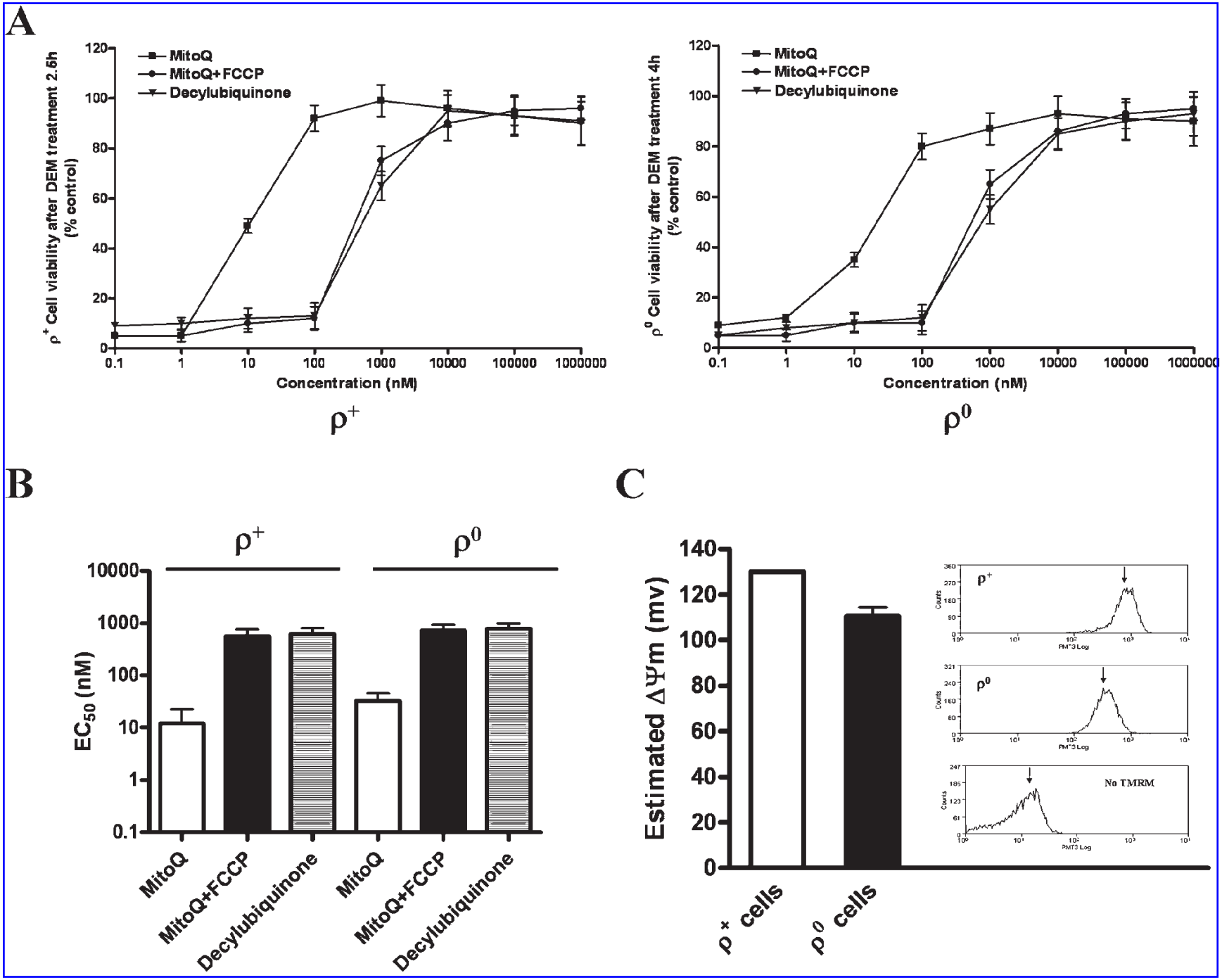
A
MitoQ
MitoQ+FCCP
Decylubiquinone
ρ+ Cell viability after DEM treatment 2.5h (% control)
Concentration (nM)
ρ+
ρ0 Cell viability after DEM treatment 4h (% control)
Concentration (nM)
ρ0
B
ρ+
ρ0
EC50 (nM)
MitoQ
MitoQ+FCCP
Decylubiquinone
MitoQ
MitoQ+FCCP
Decylubiquinone
C
Estimated ΔΨm (mv)
ρ + cells
ρ 0 cells
No TMRM

oxide and peroxynitrite and prevent lipid peroxidation, although it failed to scavenge hydrogen peroxide (13). In cell model systems, however, the antioxidant properties of MitoQ have been found to be controversial, possibly because of the use of different cell types and forms of oxidative stress (20). In this study, where oxidative stress was induced by GSH depletion, MitoQ potently inhibited ROS increase (Fig. 1C). We have previously shown that a) phase 2 enzyme induction blocks GSH-dependent oxidative stress by increasing cellular GSH levels (9), and b) nitric oxide (NO) donors prevent GSH-dependent oxidative stress by *S*-nitrosylation of redox-sensitive mitochondrial protein thiols (28). Therefore, we first examined the effects of MitoQ on cellular GSH concentration and protein thiol redox status. MitoQ did not prevent the loss of GSH induced by DEM (Table 1), but preserved the mitochondrial protein thiol redox status (Fig. 1D), indicating that the antioxidant effects of MitoQ were selective for mitochondria but not other cellular compartments and that the protective mechanism of MitoQ was similar to that of NO donors which directly protected the redox status of mitochondrial protein thiols without preserving GSH levels (28). It has been shown that MitoQ accumulates into mitochondria with the hydrophobic core of the compound inserted in the inner membrane (14). The orientation of MitoQ in the mitochondrial inner membrane and its lipophilicity may be crucial for its antioxidant properties since we have previously shown that although dUb blocks cell death after GSH depletion, ubiquinone 0 (Ub0), which lacks the hydrophobic moiety, is not protective (5). dUb is significantly more lipophilic (octanol: PBS partition coefficient $\sim 3 \times 10^5$) than Ub0 (octanol: PBS partition coefficient $\sim$ 1.0). This indicates that after GSH depletion oxidizing ROS are generated either within the lipid bilayer or at the matrix surface of the inner membrane where the CoQ_{10} moiety is adsorbed. Furthermore, the adenine nucleotide translocator (ANT) inhibitor bongkrekic acid (BgK), which also blocks GSH-dependent cell death, binds the ANT at the matrix side, further supporting the notion that MitoQ protects protein redox status from the matrix side of the inner membrane (6). Since it is known that the ANT has regulatory redox-sensitive thiol groups at the matrix surface, it is possible that MitoQ exerts its antioxidant function by protecting these groups from oxidation after GSH depletion (19).

MitoQ prevented the loss of $\Delta\psi$m (Fig. 2A and B) and preserved mitochondrial structural integrity after GSH depletion since the loss of the cristae ultrastructure, increased electron opacity, and organelle shrinkage, were effectively blocked by MitoQ (Fig. 2C). This is in line with our previous report showing that dUb, but not Ub0, also prevented these changes after GSH depletion (5). Interestingly, ρ^0 cells were relatively resistant to ROS increase, loss of $\Delta\psi$m, and cell death induced by DEM which may be the result of increased antioxidant capacity of these cells compared to the parental cell line, since SK-Hep1 ρ^0 cells possess increased levels of manganese superoxide dismutase (MnSOD) protein expression (22), and we have previously found that chronic EtBr treatment increases glutathione *S*-transferase (GST) activity in CEM cell lines (9).

The ETC is thought to be essential for the antioxidant function of MitoQ because it needs to be continuously recycled from the oxidized to reduced form in order to scavenge ROS and also because the accumulation of MitoQ into mitochondria is driven by the $\Delta\psi$m. In line with this, we found that efficacy of MitoQ was lower in ρ^0 cells (EC_{50} $\sim$30 n*M*) compared to ρ^+ cells (EC_{50} $\sim$10 n*M*). However, the efficacy of MitoQ was significantly greater in both cell lines compared to that of dUb, the nontargeted antioxidant, as well as in cells treated with MitoQ + FCCP to dissipate the $\Delta\psi$m (Fig. 4B). These results indicate that the antioxidant potential of MitoQ was highly conserved in cells lacking a functional ETC. Since MitoQ has been previously shown to be reduced by respiratory complex II (which is not encoded by mtDNA) and membrane-bound glycerol 3-phosphate dehydrogenase, but not by complex I (which is encoded by mtDNA) it may be that these enzymes serve as the major cycling mechanism for MitoQ (2, 13, 18, 25). We also showed that in ρ^0 cells, despite loss of proton pumping by the major components of the ETC, $\Delta\psi$m was estimated to be decreased only $\sim$20 mV compared to parental CEM cells (Fig. 4C). These results indicate that CEM ρ^0 cells still maintain a significant $\Delta\psi$m, in agreement with the $\Delta\psi$m determined for other ρ^0 cell lines (8, 16), sufficient to drive the accumulation of MitoQ. It has been suggested that the $\Delta\psi$m of ρ^0 cells is generated by residual mitochondrial ETC activity as well as by other ion movements such as the glycolytic ATP^{4-} to mitochondrial ADP^{3-} exchange (18).

In conclusion, we have shown that the targeted coenzyme Q derivative MitoQ protects CEM cells against GSH-dependent cell death by blocking ROS production, protein thiol oxidation, and mitochondrial permeabilization leading to caspase-independent cell death. Furthermore, we have shown that the antioxidant potential of MitoQ does not ultimately depend on a functional ETC. This research may be important in the future design of mitochondrial therapeutic antioxidants to treat diseases associated with abnormalities in the ETC and increased mitochondrial ROS production.

APPENDIX

1. Materials

All chemicals including DEM (5 m*M*) were of reagent grade and were obtained from Sigma Chemical Company (St. Louis, MO). Fluorescent probes including tetra-methyl rhodamine methyl ester (TMRM) and dichloro-dihydrofluorescein diacetate (DCFDA) were purchased from Molecular Probes (Eugene, OR). z-VADfmk (50 μM) was purchased from Sigma Chemical Company. MitoQ (500 n*M*) was from Antipodean pharmaceuticals (Auckland, New Zealand).

2. Cell culture and viability test

Human leukemic CEM cells were cultured in RPMI 1640 medium supplemented with 5% fetal bovine serum (FBS), 292 μg/ml L-glutamine, 100 U/ml penicillin, 100 μg/ml streptomycin, and 0.02 mg/ml G418. Cells were passaged daily to maintain them in log-phase growth and kept at nominal concentration of 5–8 $\times$ 10^5/ml. CEM ρ^0 cells were derived from CEM parental cells by culturing in the presence of 50 ng/ml ethidium bromide for 4 weeks, as previously described (9). ρ^0 cells were then cultured in RPMI medium with 1 m*M* pyruvate and 50 μg/ml uridine added, and regularly monitored for oxygen consumption. Cell viability was measured by trypan blue (0.2%) exclusion. Viable (trypan blue negative) and nonviable (trypan blue

positive) cells were counted using a hemocytometer, and viability was expressed as the percentage of cells excluding trypan blue.

3. Measurement of oxygen consumption, GSH, and protein thiol redox status

Oxygen consumption was measured with a Clark oxygen electrode (Oxygraph Model 5300: Yellow Spring Instrument Co., Yellow Spring, OH), as described previously (9). GSH and GSSG levels were measured using a commercial kit (Cayman Chemicals, Ann Harbor, MI); the GSH redox potential (E_h) was calculated using the modified *Nernst* equation using a cell volume as 7 μl per million cells and E_0 was taken as -240 mV (28). DTNB reactive protein thiols were determined by the method of Ellman with modification. DTNB reactive protein thiols in control were estimated after subtracting DTNB nonprotein reactive thiols (including GSH) (28).

4. Measurement of ROS production and $\Delta\psi$m

For ROS determinations, cells were pretreated with or without inhibitors for 30 min, then treated with DEM for 0, 30, 60, or 90 min, washed with phosphate-buffered saline containing 10 m*M* glucose, loaded with 10 μM DCFDA for 15 min, and analyzed immediately by flow cytometry using the FITC setting (log mode). H_2O_2 was used as a positive control for detection of cellular ROS. In each analysis, 10,000 events were recorded.

For determination of $\Delta\psi$m, cells were pretreated with or without inhibitors for 30 min, then treated with DEM for 0, 60, 120 and 180 min, washed with phosphate-buffered saline containing 10 m*M* glucose, loaded with 250 n*M* TMRM for 15 min, and analyzed immediately by flow cytometry using the PE setting (log mode). The protonophore CCCP (1 μM) was used as a control for loss of $\Delta\varphi$m. In each analysis, 10,000 events were recorded. For semiquantitative determination of $\Delta\psi$m, TMRM (40 n*M*) fluorescence was recorded for both CEM ρ^+ cells and ρ^0 cells. The $\Delta\psi$m of CEM ρ^+ cells was arbitrarily set to -130 mV and the $\Delta\psi$m of ρ^0 cells was determined using equation: $-130\text{mV} \times \log$ [fluorescence intensity of ρ^+ cells/no TMRM]/log [fluorescence intensity of ρ^0 cells/no TMRM] (24).

5. Subcellular fractionation

Subcellular fractionation was performed as described previously (29) with the following modifications. Following treatment, cells ($\sim 1 \times 10^7$) were harvested by centrifugation (600 *g* for 10 min at 4°C). Cell pellets were washed with ice-cold PBS and suspended in HEPES buffer at pH 7.4. Cells were disrupted using a $27^1/_2$ gauge needle and the cell homogenate was centrifuged at 800 *g* for 10 min at 4°C to remove nuclei and unbroken cells. The supernatant from this preparation was centrifuged at 10,000 *g* for 10 min, and the pellet was designated the 'mitochondrial' fraction while the supernatant was centrifuged at 100,000 *g* for 60 min at 4°C, and the resulting supernatant was used for preparation of cytosolic fraction. The mitochondrial and cytosolic fractions were stored at -80°C until experimentation. Protein assay was performed by Dc protein assay (Bio-Rad, Hercules CA).

6. Immunoblotting

Proteins were separated by electrophoresis on 12% SDS-PAGE gels and transferred to nitrocellulose membrane. Mouse monoclonal anti-cytochrome *c*, anti-β actin, and anti-COX II antibodies were from BD Biosciences, Pharmingen (San Diego, CA). The secondary antibody used was goat anti-mouse horseradish peroxidase-conjugated antibody, and it was purchased from BD Biosciences, Pharmingen. Chemiluminescence detection was performed using ECL detection kit according to the manufacturer's instructions (Pierce, Rockford, IL).

7. Transmission electron microscopy (TEM)

CEM cells in the logarithmic proliferation phase were pretreated with or without MitoQ for 30 min, then treated with DEM for a further 120 min (ρ^+) or 180 min (ρ^0). Cells were fixed with 2.5% glutaraldehyde in 0.1*M* cacodylate buffer, pH 7.4, at room temperature for 1 h and washed with 0.1 *M* cacodylate buffer and postfixed with 1% osmium tetraoxide in 0.1 *M* cacodylate buffer and dehydrated with graded series of ethanol, and embedded in LX112. Thin sections were prepared, and stained with uranyl acetate. Specimens were examined on a JEOL 1000X electron microscope operating at 80 KV.

8. Caspase- 3 activity assays

EnzChek®Caspase-3 Assay kits were purchased from Molecular Probes (Eugene, Oregon). CEM cell caspase-3 activity was determined using a caspase-3 synthetic fluorescent substrate. Assays were performed according to the manufacturer's instructions. Substrate cleavage increases the fluorescence which was measured using Molecular Probes fluorometer model # GEMINI XS (excitation @ 342 nm and emission @ 441 nm).

9. Statistical analysis

Data were expressed as mean $\pm$ standard deviation of the mean of three or more separate experiments performed in duplicate. ANOVA was used for significance testing ($p < 0.05$).

ACKNOWLEDGMENTS

This work was supported by National University of Singapore Grants: Academic Research Fund Grant # R183000127112 (to JSA) and Basic Medical Research Council Grant # R183000132305 (to JSA).

ABBREVIATIONS

$\Delta\psi$m, mitochondrial membrane potential; DEM, diethylmaleate; dUb, decylubiquinone; ETC, electron transport chain; GSH, glutathione; MPT, mitochondria permeability transition; ROS, reactive oxygen species; SEM, standard error of the mean.

REFERENCES

1. Adlam VJ, Harrison JC, Porteous CM, James AM, Smith RA, Murphy MP, and Sammut IA. Targeting an antioxidant to mitochondria decreases cardiac ischemia-reperfusion injury. *FASEB J* 19:1088–1095, 2005.
2. Anderson S, Bankier AT, Barrell, BG, de Bruijn, MH, Coulson AR, Drouin J, Eperon IC, Nierlich DP, Roe BA, Sanger F, Schreier PH, Smith AJ, Staden R, and Young IG. Sequence and organization of the human mitochondrial genome. *Nature* 290: 457–465, 1981.
3. Armstrong JS. Mitochondrial membrane permeabilization: the sine qua non for cell death. *Bioessays* 28: 253–260, 2006.

4. Armstrong JS and Jones DP. Glutathione depletion enforces the mitochondrial permeability transition and causes cell death in Bcl-2 overexpressing HL60 cells. *FASEB J* 16: 1263–1265, 2002.
5. Armstrong JS, Whiteman M, Rose P, and Jones DP. The Coenzyme Q10 analog decylubiquinone inhibits the redox-activated mitochondrial permeability transition: role of mitochondrial respiratory complex III. *J Biol Chem* 278: 49079–49084, 2003.
6. Armstrong JS, Yang H, Duan W, and Whiteman M. Cytochrome bc1 regulates the mitochondrial permeability transition by two distinct pathways. *J Biol Chem* 279: 50420–50428, 2004.
7. Beyer RE, Segura—Aguilar J, Di Bernardo S, Cavazzoni M, Fato R, Fiorentini D, Galli MC, Setti M, Landi L, and Lenaz G. The role of DT-diaphorase in the maintenance of the reduced antioxidant form of coenzyme Q in membrane systems. *Proc Natl Acad Sci USA* 93: 2528–-2532, 1996.
8. Buchet K and Godinot C. Functional F1-ATPase essential in maintaining growth and membrane potential of human mitochondrial DNA-depleted rho degrees cells. *J Biol Chem* 273: 22983–22989, 1998.
9. Chua YL, Zhang D, Boelsterli U, Moore PK, Whiteman M, and Armstrong JS. Oltipraz-induced phase 2 enzyme response conserved in cells lacking mitochondrial DNA. *Biochem Biophys Res Commun* 337: 375–81, 2005.
10. Costantini P, Belzacq AS, Vieira HL, Larochette N, de Pablo MA, Zamzami N, Susin SA, Brenner C, and Kroemer G. Oxidation of a critical thiol residue of the adenine nucleotide translocator enforces Bcl-2-independent permeability transition pore opening and apoptosis. *Oncogene* 19: 307–314, 2000.
11. Genova ML, Pich MM, Biondi A, Bernacchia A, Falasca A, Bovina C, Formiggini G, Castelli GP, and Lenaz G. Mitochondrial production of oxygen radical species and the role of coenzyme Q as an antioxidant. *Exp Biol Med* 228: 506–513, 2003.
12. Geromel V, Darin N, Chretien D, Benit P, DeLonlay P, Rotig A, Munnich A, and Rustin P. Coenzyme Q10 and idebenone in the therapy of respiratory chain diseases: rationale and comparative benefits. *Mol Genet Metab* 77:21–30, 2002.
13. James AM, Cocheme HM, Smith RA, and Murphy MP. Interactions of mitochondria targeted and untargeted ubiquinones with the mitochondrial respiratory chain and reactive oxygen species: Implications for the use of exogenous ubiquinones as therapies and experimental tools. *J Biol Chem* 280: 21295–21312, 2005.
14. James AM, Smith RA, and Murphy MP. Antioxidant and prooxidant properties of mitochondrial Coenzyme Q. *Arch Biochem Biophys* 423: 47–-56, 2004.
15. Jauslin ML, Meier T, Smith RA, and Murphy MP. Mitochondria-targeted antioxidants protect Friedreich Ataxia fibroblasts from endogenous oxidative stress more effectively than untargeted antioxidants. *FASEB J* 17:1972–1974, 2003.
16. Li K, Neufer PD, and Williams RS. Nuclear responses to depletion of mitochondrial DNA in human cells. *Am J Physiol* 269: C1265–1270, 1995.
17. Lin MT and Beal MF. Mitochondrial dysfunction and oxidative stress in neurodegenerative diseases. *Nature* 443: 787–795, 2006.
18. Loiseau D, Chevrollier A, Douay O, Vavasseur F, Renier G, Reynier P, Malthièry Y, and Stepien G. Oxygen consumption and expression of the adenine nucleotide translocator in cells lacking mitochondrial DNA. *Exp Cell Res* 278: 12–18, 2002.
19. McStay GP, Clarke SJ, and Halestrap AP. Role of critical thiol groups on the matrix surface of the adenine nucleotide translocase in the mechanism of the mitochondrial permeability transition pore. *Biochem J* 367:541–548, 2002.
20. Murphy MP and Smith RA. Targeting antioxidants to mitochondria by conjugation to Lipophilic cations. *Annu Rev Pharm Toxic* 47: 629–656, 2007.
21. Murphy MP. Development of lipophilic cations as therapies for disorders due to mitochondrial dysfunction. *Exp Opin Biol Therapy* 1:753–764, 2001.
22. Park SY, Chang I, Kim JY, Kang SW, Park SH, Singh K, and Lee MS. Resistance of mitochondrial DNA-depleted cells against cell death: role of mitochondrial superoxide dismutase. *J Biol Chem* 279: 7512–7520, 2004.
23. Petronilli V, Costantini P, Scorrano L, Colonna L, Passamonti S, and Bernardi P. The voltage sensor of the mitochondrial permeability transition pore is tuned by the oxidation-reduction state of vicinal thiols: Increase of the gating potential by oxidants and its reversal by reducing agents. *J Biol Chem* 269: 16638–16642, 1994.
24. Pon LA and Schon EA. *Methods in Cell Biology (Vol 65): Mitochondria*. San Diego, CA: Academic Press, 2001, p. 83–90.
25. Skowronek P, Haferkamp O, and Rodel G. A fluorescence-microscopic and flow-cytometric study of HeLa cells with an experimentally induced respiratory deficiency. *Biochem Biophys Res Commun* 187: 991–998, 1992.
26. Skulachev VP. How to clean the dirtiest place in the cell: cationic antioxidants as intramitochondrial ROS scavengers. *IUBMB Life* 57: 305–310, 2005.
27. Smith RA, Kelso GF, James AM, and Murphy MP. Targeting coenzyme Q derivatives to mitochondria. *Methods Enzymol* 382: 45–67, 2004.
28. Whiteman M, Chua YL, Zhang D, Duan W, Liou YC, and Armstrong JS. Nitric oxide protects against mitochondrial permeabilization induced by glutathione depletion: role of S-nitrosylation? *Biochem Biophys Res Commun* 339: 255–262, 2006.
29. Yang J, Liu X, Bhalla K, Kim CN, Ibrado AM, Cai J, Peng TI, Jones DP, and Wang X. Prevention of apoptosis by Bcl-2: release of cytochrome c from mitochondria blocked. *Science* 275: 1129–1132, 1997.

Address reprint requests to:
Jeffrey S. Armstrong, Ph.D
Department of Biochemistry
National University of Singapore
Kent Ridge Road
Singapore

E-mail: bchjsa@nus.edu.sg

Date of first submission to ARS Central, August 1, 2007; date of final revised submission, August 1, 2007; date of acceptance, August 12, 2007.

This article has been cited by:

1. Rommy von Bernhardi , Jaime Eugenín . 2012. Alzheimer's Disease: Redox Dysregulation As a Common Denominator for Diverse Pathogenic Mechanisms. *Antioxidants & Redox Signaling* **16**:9, 974-1031. [Abstract] [Full Text HTML] [Full Text PDF] [Full Text PDF with Links]
2. Elena Galea, Nathalie Launay, Manuel Portero-Otin, Montserrat Ruiz, Reinald Pamplona, Patrick Aubourg, Isidre Ferrer, Aurora Pujol. 2012. Oxidative stress underlying axonal degeneration in adrenoleukodystrophy: A paradigm for multifactorial neurodegenerative diseases?. *Biochimica et Biophysica Acta (BBA) - Molecular Basis of Disease* . [CrossRef]
3. Ye Feng, Xiaochuan Wang. 2012. Antioxidant Therapies for Alzheimer's Disease. *Oxidative Medicine and Cellular Longevity* **2012**, 1-17. [CrossRef]
4. Sangbin Lim, Md Abdur Rashid, Miran Jang, Yeonghwan Kim, Hyeran Won, Jeonghoon Lee, Jeong-taek Woo, Young Seol Kim, Michael P. Murphy, Liaquat Ali, Joohun Ha, Sung Soo Kim. 2011. Mitochondria-targeted Antioxidants Protect Pancreatic #-cells against Oxidative Stress and Improve Insulin Secretion in Glucotoxicity and Glucolipotoxicity. *Cellular Physiology and Biochemistry* **28**:5, 873-886. [CrossRef]
5. David J. Bonda, Xinglong Wang, George Perry, Akihiko Nunomura, Massimo Tabaton, Xiongwei Zhu, Mark A. Smith. 2010. Oxidative stress in Alzheimer disease: A possibility for prevention. *Neuropharmacology* **59**:4-5, 290-294. [CrossRef]
6. Bo Su, Xinglong Wang, David Bonda, Gorge Perry, Mark Smith, Xiongwei Zhu. 2010. Abnormal Mitochondrial Dynamics—A Novel Therapeutic Target for Alzheimer's Disease?. *Molecular Neurobiology* **41**:2-3, 87-96. [CrossRef]
7. Paula I. Moreira, Xiongwei Zhu, Xinglong Wang, Hyoung-gon Lee, Akihiko Nunomura, Robert B. Petersen, George Perry, Mark A. Smith. 2010. Mitochondria: A therapeutic target in neurodegeneration. *Biochimica et Biophysica Acta (BBA) - Molecular Basis of Disease* **1802**:1, 212-220. [CrossRef]
8. Jeffrey S. Armstrong . 2008. Mitochondria-Directed Therapeutics. *Antioxidants & Redox Signaling* **10**:3, 575-578. [Abstract] [Full Text PDF] [Full Text PDF with Links]